

Corrosion of Aluminium in Concentrated LiNO_3 Solution at High Temperature

Chunhuan Luo

Beijing Engineering Research Center for Energy Saving and Environmental Protection, University of Science and Technology Beijing, 30 Xueyuan Road, Haidian District, Beijing 100083, China
E-mail: luochunhuan@ustb.edu.cn

Received: 28 February 2015 / *Accepted:* 30 March 2015 / *Published:* 28 April 2015

The corrosion of aluminium in concentrated LiNO_3 solution at high temperature was studied with a weight loss method. The effects of concentration, temperature, pH and Li_2CrO_4 on corrosion rates were investigated. Results indicated that increasing concentration of LiNO_3 had opponent effects on aluminium corrosion. Elevating temperature and pH could increase the corrosion rate. An incompact hydroxide film was observed on the surface of aluminium in LiNO_3 solution. The corrosion was effectively depressed by adding inhibitor Li_2CrO_4 , where a compact passive film comprising $\text{Al}(\text{OH})_3$ and Cr_2O_3 may be formed. The corrosion rate of aluminium in LiNO_3 solution was much smaller than that in LiBr solution.

Keywords: Aluminium; Weight Loss; High Temperature Corrosion; SEM; XRD

1. INTRODUCTION

Absorption heat pump is a technology that can utilize renewable energy and industrial waste heat for the purpose of refrigeration and heating. In the past few years, it has been paid much attention because of its great advantages in energy conservation and environmental protection.[1-3] $\text{LiBr}/\text{H}_2\text{O}$ is generally used as the working fluid of absorption system because of its favorable thermophysical properties. However, as a traditional working fluid, $\text{LiBr}/\text{H}_2\text{O}$ has strong corrosivity to common metal materials and even corrosion resistant alloys, which not only reduces the life of absorption system, but also worsens the vacuum and the performance due to producing hydrogen and solid corrosion product.[4-10] These adverse effects restrain the applications of high-temperature absorption heat pump, such as the absorption heat transformer and triple-effect absorption refrigeration system.

In order to resolve the corrosion problem of LiBr/H₂O, abundant studies have been performed in the past few years. Adding inhibitors into LiBr aqueous solution is an economical way to reduce the corrosion. Chromate, molybdate and OH⁻ are usually utilized as the inhibitors in LiBr/H₂O absorption systems.[11-13] These inhibitors are helpful to reduce the corrosion of carbon steel and copper by forming a passive film on metal surface. Nonetheless, they still can not meet the practical requirements at high temperature, especially at a temperature above 165 °C. Some complex and organic inhibitors have also been reported.[14-16] Though Complexes inhibitors PMA/SbBr₃ and PWVA/Sb₂O₃ can further reduce the corrosion of carbon steel, the corrosion rates in 55 wt.% LiBr aqueous solution at 240 °C still reach 73.7µm/y and 120.66µm/y, respectively. Organic inhibitor benzotriazole (BTA) are effective in reducing the copper corrosion due to the formation of an insoluble and complex film, whereas its reliability is decreased with the increasing temperature of LiBr aqueous. The corrosion behaviors of high-chromium, high-molybdenum and high-nickel alloys in LiBr solution have been studied through an electrochemical method.[17-23] Though these alloys have strong corrosion resistance to general corrosion of carbon steel, the pitting corrosion still occurs in concentrated LiBr solutions at high temperature.[24-26] Moreover, the corrosion rate of Cu-Ni alloys in 65 wt. % LiBr aqueous solution at 173 °C still reaches 130.00 µm/y.[27]

As stated above, the existing inhibitors and corrosion- resisting alloys fail in settling the corrosion problem of LiBr/H₂O. In the previous research, LiNO₃/H₂O had been reported as an alternative working fluid to approach the corrosion problem. The corrosion behavior of structural material carbon steel in its concentrated solution had been investigated at high temperature.[28, 29] Results indicated that the carbon steel corrosion in LiNO₃ solution is much smaller than that in LiBr solution. Copper and aluminium, which have excellent heat-conducting property, are usually adopted as the heat exchanging materials in absorption heat pump. Because aluminium has the advantages of light quality and good economics, its corrosion behavior in concentrated LiNO₃ solution at high temperature has been investigated in this paper.

2. EXPERIMENTAL METHOD

2.1 Materials

The material for corrosion measurement is 1016 aluminium, and its chemical composition is given in Table 1. The test sample is rectangular piece (30 mm×10 mm×1 mm). Reagents of lithium nitrate (GR, >99.5 wt.%), lithium bromide (GR, >99.5 wt.%), lithium hydroxide (GR, >92.0 wt.%), and lithium chromate (AR, >98.0 wt.%) are produced by Tianjin Jinke Institute of Fine Chemicals (China). Nitric acid (AR, 65 wt.% - 68 wt.%) and acetone (AR, >99.5 wt.%) are produced by Beijing Chemical Works (China). All of them are used without further purification. The electric resistance of pure water used in this paper is 18.2 MΩ cm.

Table 1. The chemical composition of 1016 aluminium sample

composition	Si	Fe	Cu	Mn	Mg	Cr	Zn	Ti	Al
Wt. %	0.25	0.35	0.05	0.03	0.03	0.18	0.05	0.03	Balance

2.2 Apparatus and Procedure

The corrosion rate of aluminium in LiNO₃ solution was measured by weight loss method.[30, 31] The detailed experimental apparatus and procedure had been reported in the previous research.[28] Because the corrosion products on the surfaces of different metal materials were distinct, a new cleaning method was adopted in the aluminium corrosion experiment. After being rinsed with pure water and acetone, the test samples were immersed in 65 wt.% HCl for about 1 minute and were wiped with absorbent cotton softly. Then it was observed that the solid corrosion products on samples surface began to be removed. As the corrosion products were thoroughly cleaned through repeating the above operation, the samples were rinsed with pure water and acetone again, then dried at room temperature and weighed finally. The corrosion rate was calculated by the following formula: [28, 32, 33]

$$v = \frac{m_0 - m_1}{S \cdot t} \tag{1}$$

where v (g cm⁻² h⁻¹) is the corrosion rate, m_0 (g) is the mass of test sample before corrosion, m_1 (g) is the mass of test sample after cleaning corrosion product, S (cm²) is the surface area of test sample, and t (h) is the corrosion time.

The surface of test sample after corrosion was characterized by SEM/EDS (ZEISSE, Germany) and XRD (Rigaku, Japan)

3. RESULTS AND DISCUSSION

3.1 Effect of concentration of LiNO₃ on the corrosion rate

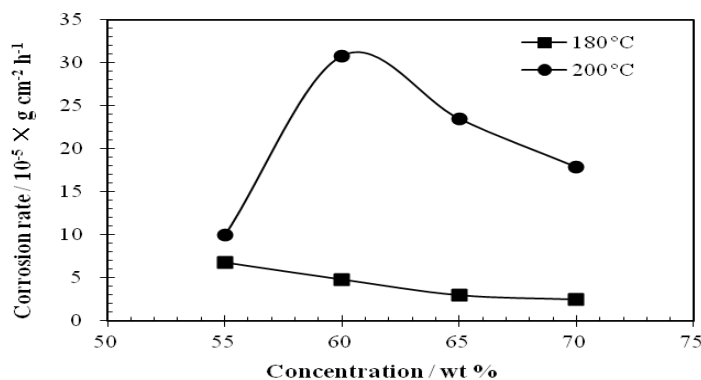


Figure 1. The effect of concentration of LiNO₃ on the corrosion rates at 180 °C and 200 °C

Fig. 1 shows the effect of concentration of LiNO₃ on the corrosion rates of aluminium in LiNO₃ solutions at pH 9.7 and at temperatures of 180 °C and 200 °C. As shown in Fig. 1, the corrosion rate of aluminium at 180 °C decreases with increasing concentration. However, the corrosion rate at 200 °C firstly increases with increasing concentration, and then decreases when the concentration is over 60 wt.%. As the concentration increases, water activity is reduced both because of the decreasing in the amount of free water and the increasing in the amount of hydration water of Li⁺ and NO₃⁻, which will depress the hydrogen evolution reaction. Meanwhile, diffusion coefficient and mass transport rate of reactants and products also decrease with increasing concentration, which will result in reducing the corrosion rate. The diffusion coefficient equation is as follow:[28, 34]

$$D_i = \frac{kT}{6\pi r_i \eta} \tag{2}$$

where D_i is the diffusion coefficient of ion, r_i is the effective radius of ion, η is the viscosity of solution, T is the absolute temperature. As the concentration increases, higher viscosity lowers the diffusion coefficient, so lowers the corrosion rate.

However, on the other hand, NO₃⁻ which has strong oxidization property is able to promote the oxidization of aluminium. Owing to the chemical erosion effect of OH⁻, a protective film is difficult to be formed on aluminium surface in alkaline solutions. So, as the concentration of NO₃⁻ increases, the anodic oxidation of aluminium will be enhanced. The cathodic reaction is as follow:[35]



From the above consideration, it is indicated that increasing concentration of LiNO₃ has opponent effects on aluminium corrosion, especially at higher temperature.

3.2 Effect of temperature of LiNO₃ solutions on the corrosion rate

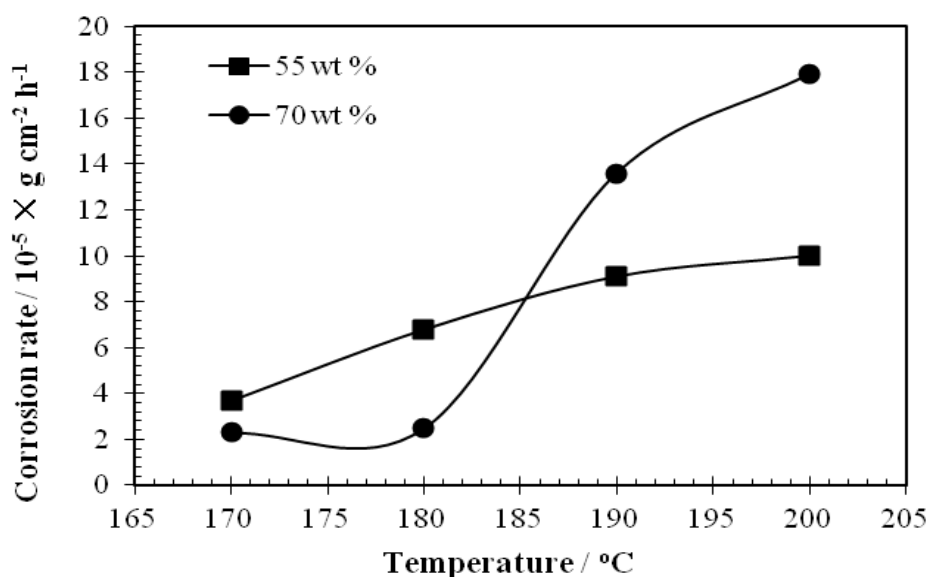


Figure 2. The effect of temperature on the corrosion rates in 55 wt.% and 70 wt.% LiNO₃ solutions

Fig. 2 gives the effect of temperature on the corrosion rates of aluminium in 55 wt.% and 70 wt.% LiNO₃ solutions at pH 9.7. As seen in Fig. 2, the corrosion rates of aluminium in different concentrations increase with increasing temperature. It is also observed that the corrosion rates of aluminium in 70 wt.% LiNO₃ solutions at 170 °C and 180 °C are less than that in 50 wt.% LiNO₃ solutions. On the contrary, as the temperatures increase to 190 °C and 200 °C, the corrosion rates in 70 wt.% LiNO₃ solutions are larger than that in 50 wt.% LiNO₃ solutions.

Based on the diffusion coefficient equation (2), the diffusion of the ions in solution and in solid corrosion product layer formed on the aluminium surface is increased with increasing temperature, so the corrosion rate is promoted by elevating temperature in both concentrations. As the aluminium samples are immersed in stronger solution at the temperature below 180°C, the decreases of water activity and ion diffusion coefficient have important influence on corrosion rate. So, the corrosion rate in 70 wt.% LiNO₃ is less than that in 50 wt.% LiNO₃ solutions. However, as the temperature increases to 190 °C, the diffusion coefficient of NO₃⁻ is further increased and its diffusion in solid corrosion product layer becomes much easier. Therefore, the concentration of NO₃⁻ has dominant influence on corrosion rate above 190 °C, and the anodic oxidation of aluminium in stronger solutions is obviously promoted.

3.3 Effect of pH of LiNO₃ solutions on the corrosion rate

Fig. 3 gives the effect of pH of LiNO₃ solutions on the corrosion rates of aluminium at various concentrations. Results show that the corrosion of aluminium at pH 9.7 is much stronger than that at pH 6.7.

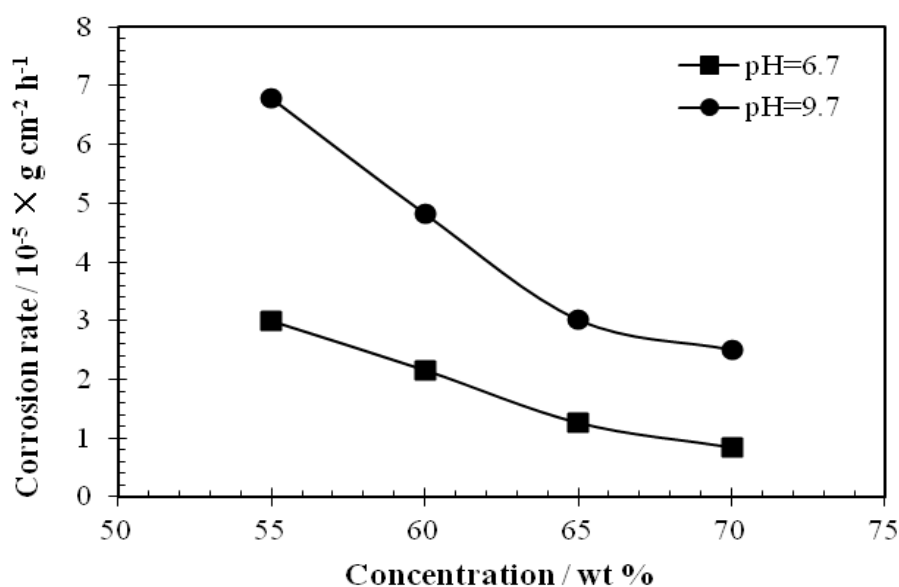


Figure 3. The effect of pH of LiNO₃ solutions on the corrosion rates varying from 55 wt.% to 70 wt.% at 180 °C

In alkaline solution, OH^- plays an important role in the chemical corrosion of aluminium, which greatly enhances the corrosion rate. Meanwhile, OH^- has destructive effect on the solid corrosion product film that is helpful to depress the mass transport rate of reactants and products. So, decreasing the pH is able to inhibit the corrosion of aluminium. However, the corrosion rates of aluminium in neutral solutions are still too larger. It is mainly because that NO_3^- also has a certain erosion effect on the solid corrosion product film through the following reactions:[36]



3.4 Effect of Li_2CrO_4 on the corrosion rate

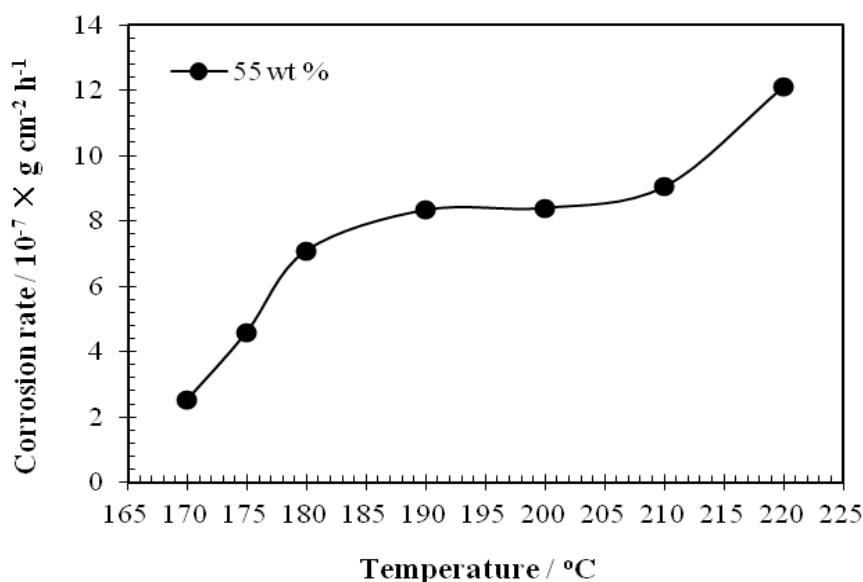


Figure 4. The effect of Li_2CrO_4 on the corrosion rates in 55 wt.% LiNO_3 solution at pH 6.7 and at temperatures from 170 °C to 220 °C

Fig. 4 gives the effect of a traditional inhibitor Li_2CrO_4 on the corrosion rates of aluminium in 55 wt.% LiNO_3 solutions at pH 6.7. As shown in Fig. 4, the corrosion rate in 55 wt.% LiNO_3 + 0.3 wt.% Li_2CrO_4 solutions at 220 °C is less than $1.21 \times 10^{-6} \text{ g cm}^{-2} \text{ h}^{-1}$. Results indicate that adding 0.3 wt.% Li_2CrO_4 is helpful to reduce the corrosion rate. It is may be due to the formation of a compact passive film on the sample surface because of the strong oxidizing property of CrO_4^{2-} , which is helpful to inhibit the aluminium corrosion. [37,38]

3.5 Comparisons with LiBr solutions

In order to compare the corrosivity of LiBr solution and LiNO_3 solution, The corrosion rates of aluminium in 55 wt. % LiBr + 0.3 wt. % Li_2CrO_4 solution at pH 6.7 were also investigated at 180 °C and 200 °C in this paper, and the comparison is given in Fig. 5. Results show that the corrosion rates of

aluminium in LiNO_3 solution are significantly smaller than that in LiBr solution. It is mainly because that the compact passive film formed on the aluminium surface is able to prevent the mass transport of NO_3^- . On the contrary, the film can not effectively prevent the diffusion of Br^- , which has strong aggressivity leading to the further erosion of aluminium.[39]

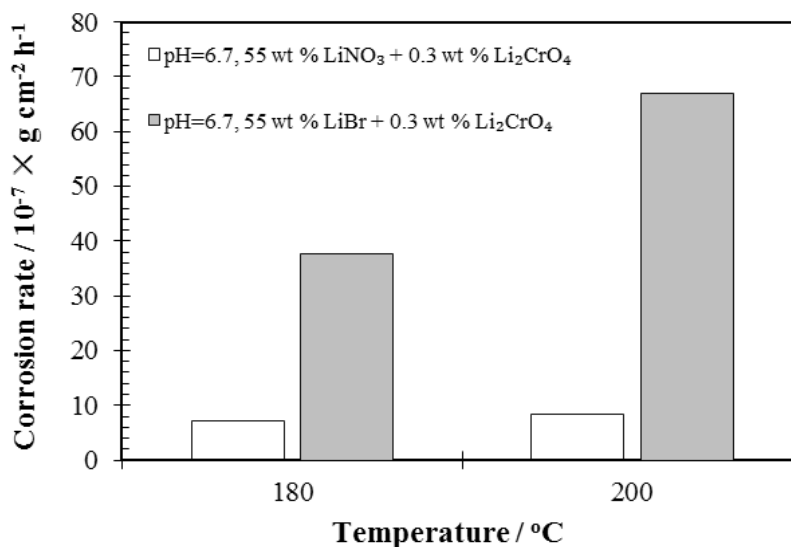


Figure 5. The comparison of aluminium corrosion in 55 wt. % LiNO_3 + 0.3 wt. % Li_2CrO_4 and in 55 wt. % LiBr + 0.3 wt. % Li_2CrO_4 at 180 °C and 200 °C

4. SURFACE ANALYSIS

4.1 Analysis of corrosion surface morphologies

In order to further investigate the influence of inhibitor Li_2CrO_4 on aluminium corrosion. The surface morphologies of the samples immersed in 55 wt.% LiNO_3 and 55 wt.% LiNO_3 + 0.3 wt. % Li_2CrO_4 solutions at pH 6.7 and 180 °C for 200 h have been characterized by SEM, and the results are exhibited in Fig.6.

As seen in Fig. 6a and c, a thick and loose solid corrosion products layer is formed on the surface of aluminium sample in 55 wt.% LiNO_3 solution. On the contrary, a thin film is observed on the sample surface in 55 wt.% LiNO_3 + 0.3 wt. % Li_2CrO_4 solution, and the solid corrosion products are distributed homogeneously. By comparing Fig. 6b and d, it is clear that the morphology of the sample surface in LiNO_3 solution without Li_2CrO_4 is incompact, which is less protective to corrosion. However, a compact passive film is formed on the surface of aluminium sample immersed in LiNO_3 solution with Li_2CrO_4 .

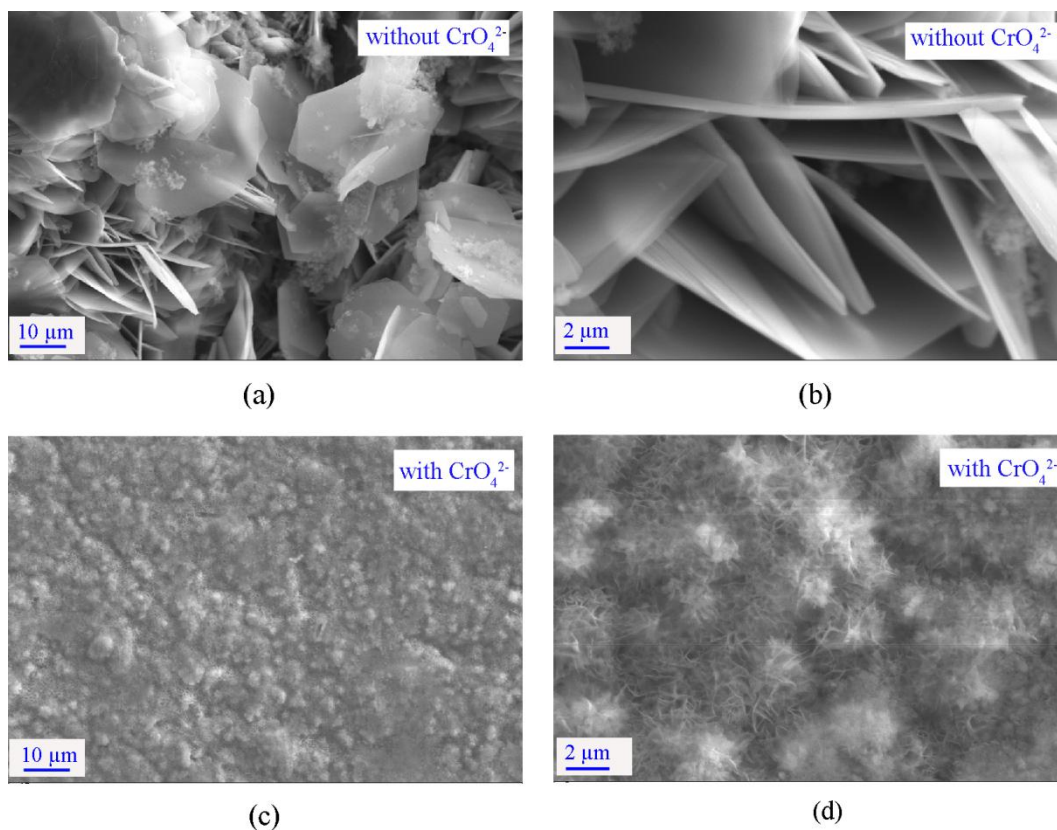


Figure 6. SEM micrograph of surface of aluminium in 55 wt. % LiNO₃ solution and 55 wt. % LiNO₃ + 0.3 wt. % Li₂CrO₄ solution at pH 6.7 and 180 °C for 200 h

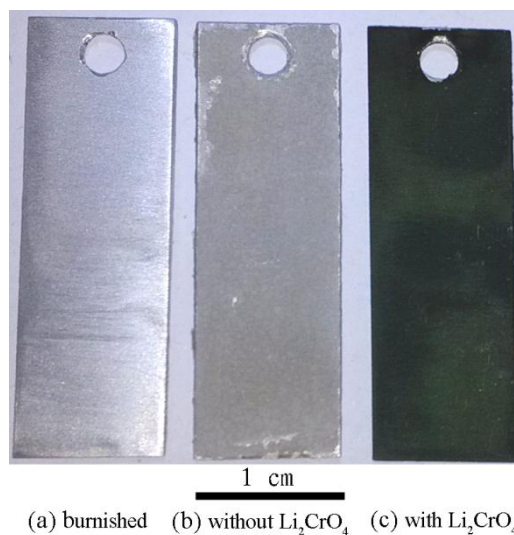


Figure 7. Digital images of aluminium specimens

Fig.7 shows the digital images of aluminium specimens. It is also found that a green compact film is tightly covered on the surface of aluminium specimen in LiNO₃ solution with Li₂CrO₄, which can effectively depress the mass transport of reactants and products. Therefore, the inhibitor Li₂CrO₄ is

effective for inhibiting aluminium corrosion, and this agrees well with the results of weight loss experiment.

4.2 Analysis of corrosion products

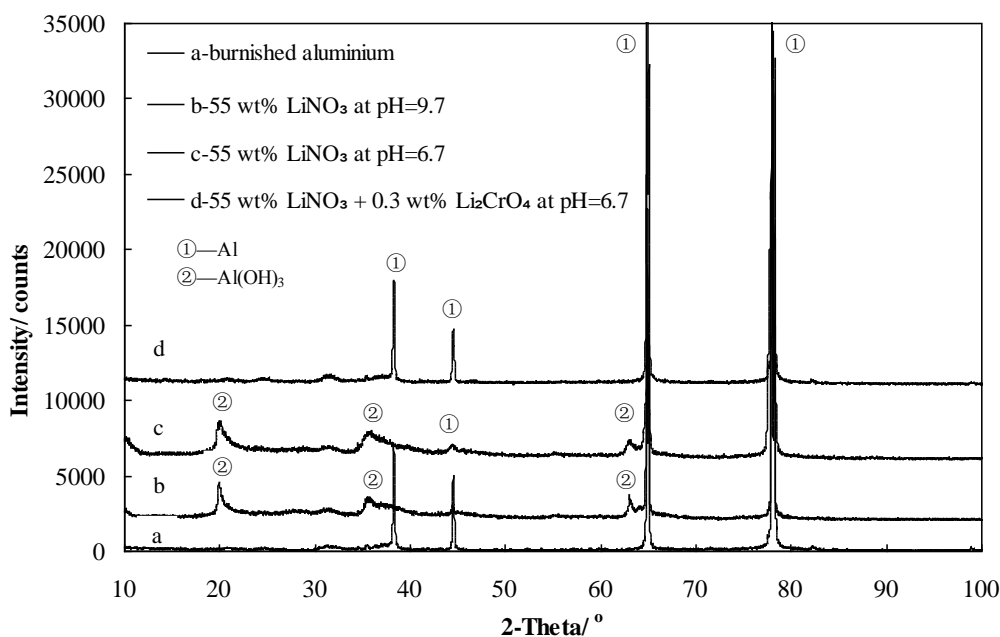
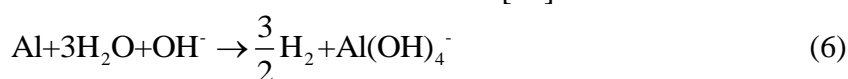


Figure 8. XRD pattern of surface of aluminium specimens

The corrosion products on aluminium sample were characterized by SEM/EDS and XRD. The XRD patterns are exhibited in Fig. 8, where a is the spectrum of the surface of aluminium burnished; b is the spectrum of the surface of aluminium immersed in 55 wt. % LiNO₃ solution at pH 9.7 and 180 °C for 200 h; c is the spectrum of the surface of aluminium in 55 wt. % LiNO₃ solution at pH 6.7 and 180 °C for 200 h; d is the spectrum of the surface of aluminium in 55 wt. % LiNO₃ + 0.3 wt. % Li₂CrO₄ solution at pH6.7 and 180 °C for 200 h.

By comparing XRD spectrum a, b and c, it is proved that a hydroxide film is formed on the aluminium surface immersed in 55 wt. % LiNO₃ solution at pH 6.7 and 9.7. The corrosion products at various pH values are identical, whereas the mechanisms for the anodic oxidation of aluminium are different.

In alkaline solutions, the corrosion of aluminium can be divided into chemical dissolution and electrochemical reactions. Al(OH)₄⁻ which is the only stable form of aluminium in alkaline solution is produced in the chemical dissolution reaction:[40]



This direct chemical dissolution of the aluminium metal is very intense, which leads to a high corrosion rate in the early stage of corrosion. As a competing process, the partial electrochemical reactions also occur on aluminium surface. A hydroxide film is formed by the anodic oxidation of

aluminium. Hydrogen and ammonia gas are produced via the cathodic reduction reactions of H^+ and NO_3^- . The electrochemical reactions are as follows: [41, 42]

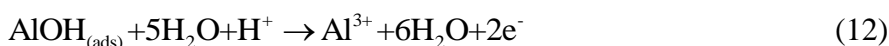


As the hydroxide film grows, the direct chemical dissolution of aluminium should be inhibited due to depressing the inward diffusion of OH^- . After that, the anodic oxidation of aluminium becomes the dominant corrosion. Because $Al(OH)_3$ is not thermodynamically stable in alkaline solution, it will be dissolved by OH^- at the hydroxide film/solution interface. The further corrosion of aluminium is result from the film dissolution reaction: [43]



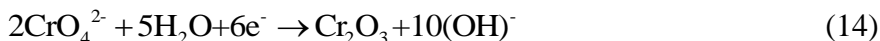
Therefore, the aluminium corrosion in alkaline solution is mainly caused by direct chemical dissolution and indirect electrochemical dissolution by consecutive hydroxide film formation and dissolution.

In neutral solutions, the direct chemical dissolution of aluminium can never occur. Aluminium dissolution is due to the following reactions: [44]



Reactions (11) and (12) are the general mechanism for aluminium dissolution. Based on this reaction scheme, it is indicated that water activity plays an important role in the process of aluminium dissolution. As Al^{3+} ion is ejected from the base metal, it will easily react with OH^- which is produced in the cathodic reduction reactions of H^+ and NO_3^- . So, a hydroxide film is also formed on the surface of aluminium in neutral solutions.

As shown in spectrum a and d, there is only peaks of Al in the XRD spectrum of corrosion products on aluminium sample immersed in 55 wt. % $LiNO_3$ + 0.3 wt. % Li_2CrO_4 solution at 180 °C and pH 6.7. It is probably because the corrosion film is too thin to be detected. However, by means of SEM/EDS, peaks of elements of O, Al and Cr have been observed in the EDS spectrum, which means that these elements are contained in the thin film. Therefore, it could be concluded that a thin and compact passive film comprising of $Al(OH)_3$ and Cr_2O_3 is formed on the aluminium surface. The cathodic reaction of CrO_4^{2-} is shown as follow:



5. CONCLUSIONS

The effects of concentration, temperature, pH and inhibitor Li_2CrO_4 on the corrosion rates of aluminum in $LiNO_3$ solution were investigated at high temperature. The surface and corrosion products of aluminum samples immersed in $LiNO_3$ solution was analyzed by XRD and SEM/EDS. The

corrosivity of LiNO_3 solution has been also compared with that of LiBr solution. The main conclusions are shown as follows:

(1) Increasing concentration of LiNO_3 has opponent effects on aluminium corrosion. In stronger solution, NO_3^- ion which has strong oxidization property will promote the oxidization of aluminium. However, the decreases of water activity and viscosity of solution will depress the corrosion.

(2) The corrosion rate is increased with the increasing temperature through promoting the diffusion of ions. Elevating temperature has a greater influence on the corrosion rates in stronger LiNO_3 solutions.

(3) The corrosion rate of aluminium in neutral solution is much less than that in alkaline solution. It is because that chemical dissolution of aluminium can never occur in the former solution.

(4) In LiNO_3 solution, an incompact hydroxide film is formed on the surface of aluminium, while in LiNO_3 solution with addition of Li_2CrO_4 , a compact passive film comprising of $\text{Al}(\text{OH})_3$ and Cr_2O_3 may be formed, which can effectively inhibit aluminium corrosion.

(5) The corrosion of aluminium in LiNO_3 solution is much less than that in LiBr solution.

So, considered from the aspect of corrosion, LiNO_3 solution has a great potential in the field of high-temperature absorption heat pump.

ACKNOWLEDGEMENTS

The author gratefully acknowledge financial support from the Fundamental Research Funds for the Central Universities (No.: FRF-TP-14-022A1) and China Postdoctoral Science Foundation (No.: 2014M560049).

References

1. D. C. Alarcón-Padilla, L. García-Rodríguez, *Desalination*, 212 (2007) 294.
2. J. Woods, J. Pellegrino, E. Kozubal and J. Burch, *J. Membrane Sci.*, 378 (2011) 85.
3. F. T. Sun, L. Fu, J. Sun and S. G. Zhang, *Energy*, 69 (2014) 516.
4. K. Tanno, S. Saito, M. Itoh and A. Minato, *Boshoku Gijutsu*, 33 (1984) 516.
5. R. Sánchez-Tovar, M. T. Montañés and J. García-Antón, *Corros. Sci.*, 60 (2012) 118.
6. M. J. Muñoz-Portero, J. García-Antón, J. L. Guiñón and V. Pérez Herranz, *Corrosion*, 62 (2006) 1018.
7. R. M. Fernandez-Domene, R. Sánchez-Tovar and J. García-Antón, *J. Electrochem. Soc.*, 161 (2014) C565.
8. R. Leiva-García, M. J. Muñoz-Portero and J. García-Antón, *ECS Trans.*, 41 (2012) 45.
9. W. Rivera, R. J. Romero, M. J. Cardoso, J. Aguillón and R. Best, *Int. J. Energ. Res.*, 26 (2002) 747.
10. M. Itagaki, Y. Hirata and K. Watanabe, *Corros. Sci.*, 45 (2003) 1023.
11. K. Tanno, M. Itoh, T. Takahashi, H. Yashiro and N. Kumagai, *Corros. Sci.*, 34 (1993) 1441.
12. K. Tanno, M. Itoh, H. Sekiya, H. Yashiro and N. Kumagai, *Corros. Sci.*, 34 (1993) 1453.
13. A. Igual Muñoz, J. García-Antón, J. L. Guiñón and V. Pérez Herranz, *Electrochim. Acta*, 50 (2004) 957.
14. X. Hu, C. Liang and N. Huang, *J. Iron. Steel. Res. Int.*, 13 (2006) 56.
15. X. Hu, C. Liang, *Mater. Chem. Phys.*, 110 (2008) 285.

16. M. Finšgar, I. Milošev, *Corros. Sci.*, 52 (2010) 2737.
17. R. M. Fernández-Domene, E. Blasco-Tamarit, D. M. García-García and J. García-Antón, *Corros. Sci.*, 55 (2012) 40.
18. R. Sánchez-Tovar, M. T. Montañés and J. García-Antón, *Corros. Sci.*, 60 (2012) 118.
19. A. Igual-Muñoz, J. García-Antón, J. L. Guiñón and V. Pérez Herranz, *Corros. Sci.*, 49 (2007) 3200.
20. D. Itzhak, T. Greenberg, *Corrosion*, 55 (1999) 795.
21. A. Igual Muñoz, J. García-Antón and J. L. Guiñón, *Corrosion*, 59 (2003) 32.
22. E. Martínez Meza, J. Uruchurtu Chavarin and J. Genesca Liongeras, *Corrosion*, 65 (2009) 461.
23. D. M. García- García, J. García-Antón, A. Igual Muñoz and E. Blasco-Tamarit, *Corrosion*, 63 (2007) 462.
24. M. Kaneko, H. S. Isaacs, *Corros. Sci.*, 50 (2008) 1848.
25. G. Lothongkum, S. Chaikittisilp and A. W. Lothongkum, *Appl. Surf. Sci.*, 218 (2003) 202.
26. M. Kaneko, H. S. Isaacs, *Corros. Sci.*, 44 (2002) 1825.
27. N. Huang, C. Liang and D. Tong, *T. Nonferr. Metal. Soc.*, 12 (2002) 424.
28. C. Luo, Q. Su, *Corros. Sci.* 74 (2013) 290.
29. C. Luo, Q. Su and W. Mi, *Int. J. Refrig.*, 36 (2013) 1689.
30. S. Jiangzhou, R. Z. Wang, *Appl. Therm. Eng.*, 21(2001) 1161.
31. C. Liang, X. Hu, *J. Iron. Steel. Res. Int.*, 15 (2008) 49.
32. H. Zarrok, A. Zarrooouk, B. Hammouti, R. Salghi, C. Jama and F. Bentiss, *Corros. Sci.*, 64 (2012) 243.
33. Y. G. Avdeev, Y. I. Kuznetsov and A. K. Buryak, *Corros. Sci.*, 69 (2013) 50.
34. Q. X. Cha, *Introduction to Kinetics of Electrode Processed*, Science Press, Beijing (2002).
35. T. H. Nguyen, R. T. Foley, *J. Electrochem. Soc.*, 127 (1980) 2563.
36. S. I. Pyun, S. M. Moon, S. H. Ahn and S. S. Kim, *Corros. Sci.*, 41 (1999) 653.
37. G. Mu, T. Zhao, *Journal of Chinese Society of Corrosion and Protection*, 8 (1988) 335.
38. M. A. Ramirez-Arteaga, J. G. Gonzalez-Rodriguez, E. Sarmiento-Bustos and I. Rosales, *Int. J. Electrochem. Sci.*, 9 (2014) 161.
39. C. Liang, X. An, *Refrigeration*, 19 (2000) 23.
40. J. S. Zhang, M. Klasky and B. C. Letellier, *J. Nucl.Mater.*, 384 (2009) 175.
41. S. M. Moon, S. I. Pyun, *Corros. Sci.*, 39 (1997) 399.
42. S. M. Moon, S. I. Pyun, *Electrochim. Acta*, 44 (1999) 2445.
43. S. M. Moon, S. I. Pyun, *J. Solid State Electr.*, 3 (1998) 156.
44. I. B. Obot, N. O. Obi-Egbedi, S. A. Umoren and E. E. Ebenso, *Int. J. of Electrochem. Sc.*, 5 (2010) 994.